

Implementation of Finite Element Method for Prediction of Soil Liquefaction Around Underground Structure

Dr. Mohammed Y. Fatah

Building and Construction Engineering Department, University of Technology/Baghdad

Dr. Mohammed A. Al-Neami 

Building and Construction Engineering Department, University of Technology/Baghdad

Nora Hameed Jajjawi

Building and Construction Engineering Department, University of Technology/Baghdad

Received on: 10/1/2012 & Accepted on: 4/10/2012

ABSTRACT

Liquefaction is the rapid loss of shear strength in cohesionless soils subjected to dynamic loading, that it is a state of saturated cohesionless soil when its entire shear strength is reduced to zero due to pore water pressure caused by vibration. Liquefaction depends on the nature, magnitude and type of dynamic loading. An entire stratum may be liquefied at the same time under shock loading, or liquefaction may start at the top and proceed downward with steady-state vibrations.

In this paper, finite element method is used in an attempted to study liquefaction of soil based on the case solved previously by transient infinite element for 2D soil - structure interaction analysis considering infinite boundaries but without generation of pore water pressure. The properties of fully saturated sandy soil and concrete are fed to geotechnical finite element software called QUAKE/W program.

The results showed that liquefaction occurs faster at shallow depths due to low overburden pressure. Also, liquefaction zones and deformation occur faster with the increase of dynamic loading amplitude. The analysis marked that increasing the amplitude pressure accelerates the occurrence of initial liquefaction and increases the pore water pressure.

Keywords: liquefaction, QUAKE/W program, sand deformation, underground structure.

توظيف طريقة العناصر المحددة في تخمين تسهيل التربة حول منشأ تحت الارض

الخلاصة

يعرف التسييل بأنه فقدان السريع في مقاومة القص للتربة عديمة التماسك المعرضة الى حمل ديناميكي وهذا يعني انه حاله للتربة عديمة التماسك المشبعة عندما تنخفض مقاومتها للقص الى الصفر نتيجة ارتفاع ضغط ماء المسام الذي تسببه الاهتزازات. يعتمد التسييل بطبيعته على مقدار ونوع الحمل الديناميكي , ويمكن لطبقة التربة بكاملها ان تسيل في نفس الوقت عند تعرضها لحمل صدمه او يمكن ان يبدأ التسييل في قمة الطبقة ثم ينتقل الى اسفلها عند تعرضها الى اهتزازات منتظمة.

٧٠٣

في هذا البحث استعملت طريقة العناصر المحددة في محاولة لدراسة تسهيل التربة بناءً على مسألة محلولة سابقاً لتحليل ثنائي الأبعاد للتداخل بين التربة والمنشأ باستعمال العناصر اللامنتهية المنتقلة (transient) بدون تولد ضغط ماء المسام. وتم تغذية خواص التربة الرملية المشبعة والخرسانة إلى برنامج حاسبة يستعمل لتحليل المسائل الجيوتكنيكية بطريقة العناصر المحددة يسمى QUAKE/W. لقد بينت النتائج أن التسهيل يحدث أسرع في أعماق ضحلة نتيجة قلة ضغط تثقل التربة وكذلك تحدث مناطق التسهيل والتشوهات بشكل أسرع مع زيادة القيمة القصوى للحمل الديناميكي. وقد أشارت النتائج إلى أن زيادة القيمة القصوى للضغط المسلط يعجل من حدوث التسهيل الأولي ويزيد قيمة ضغط ماء المسام.

INTRODUCTION

Liquefaction is a physical process that takes place during some earthquakes. Liquefaction may lead to ground failure. As a consequence of liquefaction, water-saturated, well sorted, fine grained sands and silts behave as viscous fluids. This behaviour is very different than solids behaviour. Liquefaction takes place when seismic shear waves pass through a saturated granular soil layer. These shear waves distort the soils granular structure, and cause some of its pore spaces to collapse. The collapse of the granular structure increases pore space water pressure. Furthermore, it also decreases the soil's shear strength. If pore space water pressure increases to the point where the soil's shear strength can no longer support the weight of the overlying soil, buildings, roads, houses, etc., then the soil will flow like a liquid. Consequently, extensive surface damage results.

POUR WATER PRESSURE BUILD-UP IN SATURATED SOILS

Extensive research had been performed in which laboratory specimens of saturated sand under zero driving shear stresses are subjected to either controlled cyclic stresses or strains. Many variables have been investigated including density of the sand, confining pressure, frequency of loading, shape of load cycle, method of sample preparation and cyclic loading history. Excess pore water pressure may build up under cyclic loading conditions that cause the effective stress to decrease. When soil is under an is tropically consolidated condition, the effective stress may reduce to zero when the excess pore water pressure continuously builds up. Seed and Lee (1966) defined initial liquefaction as a point at which the increase of excess pore water pressure is equal to the initial confining stress.

A number of approaches and a large amount of laboratory tests have been conducted on the liquefaction potential and prediction of the excess pore water pressure under earthquake loading conditions. One important and commonly accepted approach is the cyclic stress method developed by Seed et al., (1976). In this method, the earthquake loading, expressed in terms of equivalent cyclic shear stress, is compared with the liquefaction resistance of the soil, also expressed in terms of cyclic shear stress. When the earthquake loading exceeds the resistance, liquefaction or maximum excess pore water pressure is expected to occur. The level of excess pore water pressure development can also be predicted based on the cyclic stress approach in which the excess pore water pressure is directly related to the amplitude of cyclic stress and the number of the stress cycles. Figure (1) illustrates a typical normalized relationship between the cyclic ratio and the pore pressure ratio. The cyclic ratio is the ratio of the number of cycles applied N divided by the number of cycles required for liquefaction N_L ; that is, N/N_L .

PREVIOUS ANALYSES OF SOIL DYNAMICS PROBLEMS

Amini and Duan (2002) described a numerical model which is used to study the soil liquefaction resistance at high confining pressures. A two-dimensional numerical model was set up. Base accelerations with different magnitudes and frequencies were applied to the model. The pore water pressure and effective stress at different depths in the model were monitored during shaking. It was found that, soil liquefaction resistance increases with the increasing of confining pressure at large depths. At a large acceleration magnitude, liquefaction can occur at virtually any depth. It was concluded that at a lower frequency, liquefaction occurred faster at large depths.

Ashford et al. (2004) described a pilot test program that was carried out to determine the appropriate charge weight, delay, and pattern required to induce liquefaction for full-scale testing of deep foundations. The results of this investigation confirmed that controlled blasting techniques could successfully be used to induce liquefaction in a well-defined, limited area for field-testing purposes. The tests also confirmed that liquefaction could be induced at least two times at the same site with nearly identical results. Excess pore pressure ratios greater than 0.8 were typically maintained for at least 4 minutes after blasting. The test results indicated that excess pore pressure ratios produced by blasting could be predicted with reasonable accuracy when single blast charges were used.

Sitharam et al. (2004) studied methods of determining the dynamic properties as well as potential for liquefaction of soils. Parameters affecting the dynamic properties and liquefaction have been brought out. A simple procedure of obtaining the dynamic properties of layered ground has been highlighted. Results of a series of cyclic triaxial tests on liquefiable sands collected from the sites close to the Sabarmati river belt have been presented. Simple method was used to obtain the equivalent modulus of layered system. Cyclic strain-controlled triaxial tests to evaluate the dynamic properties and liquefaction potential of sands have been carried out. It has been brought out that the material immediately beneath the foundation plays a dominant role in controlling the dynamic response.

It can be concluded from previous studies on liquefaction that most of them concentrated on earthquake induced liquefaction and that little studies dealt with liquefaction caused by mechanical factors. Some equipment or heavy machines used during construction particularly on saturated sandy soil might cause some vibration and consequently, a loose soil will be ready for liquefaction.

DESCRIPTION OF THE PROBLEM

A half-space with an open rectangular mine shown in Figure (2) is considered. This case was solved by Yerli et al. (1998) using transient infinite elements (TIE) and Dawood (2006) using mapped infinite elements without considering development of pore water pressure. It is assumed that, a 15.24 cm thick concrete lining is added on the surface of the open-mined space so that, the inside dimensions of the opening remain the same as in the unsupported case. The material properties of the half-space are shown in Table (1).

Under the effect of the loading condition shown in Figure (2), the plane strain problem is solved by the finite element method. The finite element mesh is shown in

Figure (3). This problem is analyzed for time period equals (0.075 sec) with ($\Delta t = 0.0002$ sec) which means (375) time steps.

COMPUTER PROGRAM

The program QUAKE/W, (2004) is a geotechnical finite element software product used for the dynamic analysis of earth structures subjected to earthquake shaking and other sudden impact loading. QUAKE/W is part of GeoStudio and is, consequently, the integration of QUAKE/W and other products within GeoStudio greatly expands the type and range of problems that can be analyzed beyond what can be done with other geotechnical dynamic analysis software. It is formulated for two-dimensional plane strain problems. QUAKE/W program can be used as a stand alone product, but one of its main attractions is the integration with the other GeoStudio products, (Manual of Dynamic Modeling of QUAKE/W, 2009).

PORE - PRESSURE FUNCTION

The pore-pressures generated during earthquake shaking are a function of the equivalent number of uniform cycles, N , for a particular earthquake and the number of cycles, N_L , which will cause liquefaction for a particular soil under a particular set of stress conditions. The ratio of N/N_L is then related to a pore-pressure parameter r_u as shown in Figure (4).

In the program QUAKE/W, N_L is obtained from the cyclic number function, and therefore, a cyclic number function must be attached to the pore pressure function. QUAKE/W computes the pore-pressure from the equation:

$$u_e = r_u \times \sigma'_{3(\text{static})} \quad \dots(1)$$

where :

u_e = Excess pore water pressure,

r_u = Pore water pressure ratio, and

$\sigma'_{3(\text{static})}$ = Effective minor principle stress.

The same problem is solved here by the program QUAKE /W using linear elastic model. Eight node quadrilateral isoparametric elements are used. In order to study the pore water pressure changes under such loading condition, the soil is assumed to be saturated; i.e. the water table is located at the ground surface. The vertical displacement at points A, B, and C are presented in Figure (5a). For comparison purposes, the results obtained by Yerli et al. (1998) and Dawood (2006) are presented in Figure (5b) and Figure (5c) respectively.

It is seen that, the vertical displacement of point (A) shows very good agreement with the results of both Yerli et al. (1998) and Dawood (2006). For point B, The displacement values agree more with those of Dawood (2006) rather than those of Yerli et al. (1998). For the displacements at point C, good agreement was obtained with Yerli et al. (1998) and Dawood (2006). The pore water pressure time history at points D, E, and F (see Figure 3) located at depths 2, 4 and 6 m respectively are presented in Figure (6). It can be noticed that, the pore water pressure increases with time at the three points and that initial liquefaction takes place at point D faster than other points. This means that, liquefaction takes place first at shallow depths due to low overburden pressure. Figure (7) shows the surface displacement at different

times, while Figure (8) shows the liquefaction zones at time (0.075 sec), and Figure (9) shows the contour lines of pore water pressure. It can be noticed from Figure (7) that, the maximum displacement is greater directly below the load and that the displacement continues to increase despite that the load effect has been vanished at time ($t = 0.01$ sec.) which clarifies the stage of free vibration of the system.

The same problem was extended to study the effect of amplitude pressure on the dynamic response. The vertical displacement at points A, B, and C are presented in Figure (10) under the effect of amplitude pressure of 766 kPa. The pore water pressure time history at points D, E, and F is presented in Figure (11). Figure (12) shows the vertical displacement at points A, B, and C for an amplitude pressure of 1150 kPa. The pore water pressure time history at points D, E, and F is presented in Figure (13) while Figures (14) and (15) show the liquefaction zones at time (0.075 sec) around underground opening under $P_0 = 766$ kPa and 1150 kPa, respectively. Figure (16) shows the relationship between the maximum pulse pressure and the predicted surface displacement while Figure (17) presents the relation between the maximum pulse pressure and the maximum pore water pressure generated around the underground opening. From Figures (10) and (12), it can be noticed that increasing the amplitude pressure from (383.1) kPa in Dawood study to (766) kPa and then to (1150) kPa at point A leads to increase in the vertical displacement of about (100) % and (150) %, respectively. The same increase in the amplitude pressure accelerates the occurrence of initial liquefaction; for example, the time for initial liquefaction at point E decreases from 0.06 sec. to about 0.008 sec. due to this increase in amplitude pressure.

In addition, liquefaction zones extend to areas around the underground opening when the amplitude pressure increased. Figure (17) reveals that, the increase of pore water pressure due to increase of amplitude pressure reaches a plateau above which there is no evident increase.

CONCLUSIONS

The following conclusions can be drawn from the study:

1. The comparison between results obtained from finite element method with previous analyses showed clear superiority and accuracy of the program QUAKE/W concerning the liquefaction zones in sandy soils; it can be used successfully to examine the effect of several parameters on liquefaction and the interrelationships between them.
2. Liquefaction occurs faster at shallow depths due to low overburden pressure. Liquefaction mostly occurs within the top 10 m below the ground surface, although, it can occur up to about 20 m deep.
3. Liquefaction and deformation occur faster with the increase of loading amplitude increasing the amplitude pressure accelerates the occurrence of initial liquefaction and increases the pore water pressure.
4. Liquefaction zones increase with the increase of load amplitude. Tracing the propagation of liquefaction zones, one can notice that liquefaction occurs first near the loading end and then develops faraway.

REFERENCES

- [1]. Amini, F., Duan, Z., (2002), "Centrifuge and Numerical Modeling of Soil Liquefaction at Very Large Depths", 15th ASCE Engineering Mechanics Conference, Columbia University New York, NY.

- [2]. Ashford, S.A., Rollins, K.M. and Lane, J.D., (2004), "Blast-Induced Liquefaction for Full-Scale Foundation Testing", *Journal of Geotechnical and Geo-environmental Engineering*, ASCE, Vol. 130, No.8, p.p. 798-806.
- [3]. Dawood, S.H. (2006), "Dynamic Analysis of Soil Structure Interaction Problems Considering Infinite Boundaries", M.Sc. Thesis, University of Technology, Iraq.
- [4]. Manual of Dynamic Modeling with QUAKE/W, (2009). "An Engineering Methodology", 4th Edition, Geo-Slope International, Ltd.
- [5]. Seed, H.B. and Lee, K.L., (1966), "Liquefaction of Saturated Sand during Cyclic Loading", *Journal of Soil Mechanics and Foundations Division*, ASCE, Vol.92, SM6, p.p.105-134
- [6]. Seed, H.B., Martin, P.P. and Lysmer, J., (1976), "Pore-Water Pressure Changes during Soil Liquefaction", *Journal of the Geo-technical Engineering Division*, ASCE, GT4, p.p.323-345.
- [7]. Seed, H.B., and Booker, J.R., (1977), "Stabilization of Potentially Liquefiable Sand Deposits Using Gravel Drains", *Journal of Geotechnical Engineering Division*, ASCE, Vol. 103, No., GT7, p.p.757-768.
- [8]. Sitharam, T.G., Govinda Raju, L. and Sridharan, A., (2004), "Dynamic Properties and Liquefaction Potential of Soils", *Journal of Current Science*, Vol. 87, No. 10, 25, November.
- [9]. Yerli, H.R., Temel, B. and Kiral, E., (1998), "Transient Infinite Elements for 2D Soil-Structure Interaction Analysis", *Journal of Geotechnical and Geo-environmental Engineering ASCE*, Paper No. 13807, Vol. 124. No.10.

**Table (1) – Material properties of the soil and concrete for the problem
(from Yerli et al., 1998).**

Material Properties	Soil	Concrete
Shear modulus, G (N/m ²)	470.24×10^6	10622.0×10^6
Poisson's ratio, ν	0.10	0.17
Unit weight, γ_t (kN/m ³)	20.48	22.63

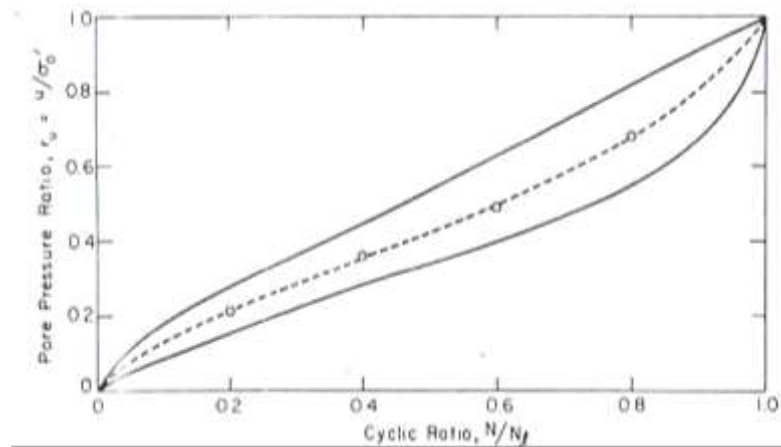


Figure (1) – Rate of pore water pressure build up in cyclic simple shear test (Seed et al., 1976).

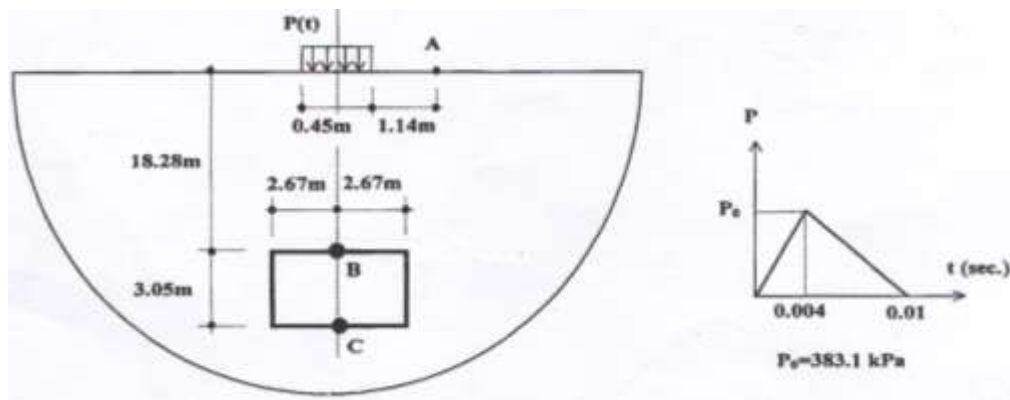


Figure (2) – Underground opening and forcing function for the problem (from Dawood, 2006).

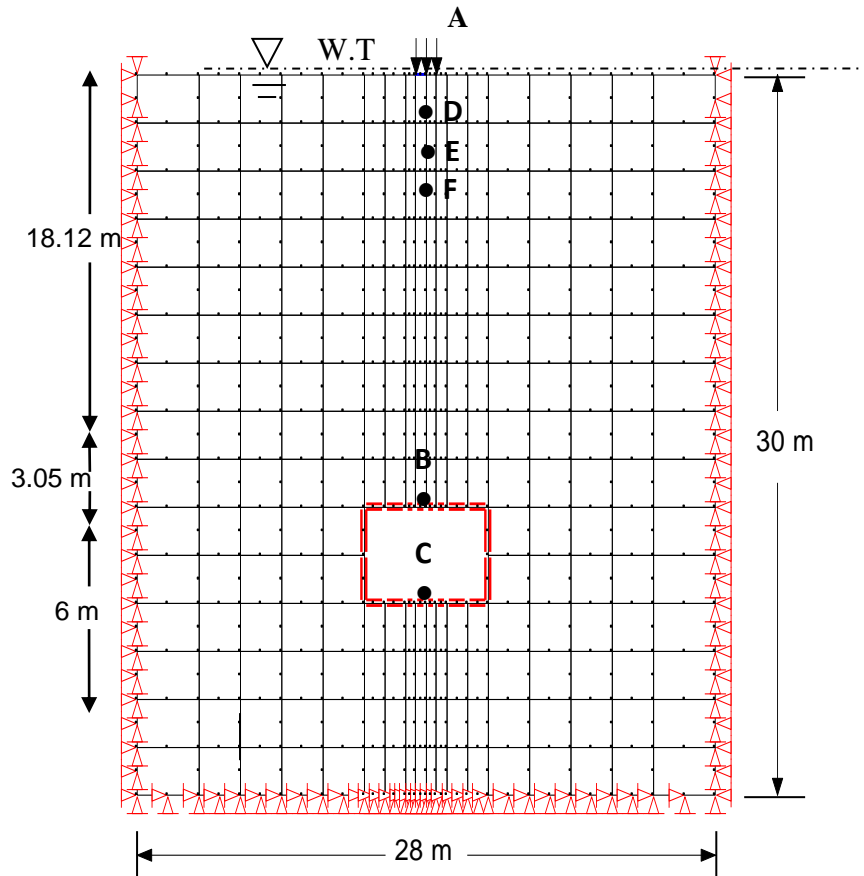


Figure (3) – Finite element mesh for the underground opening problem.

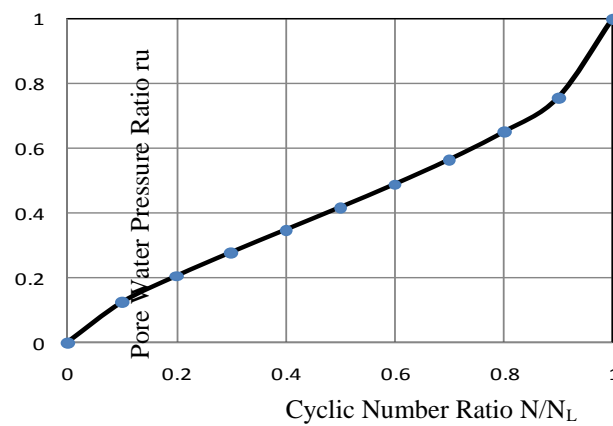
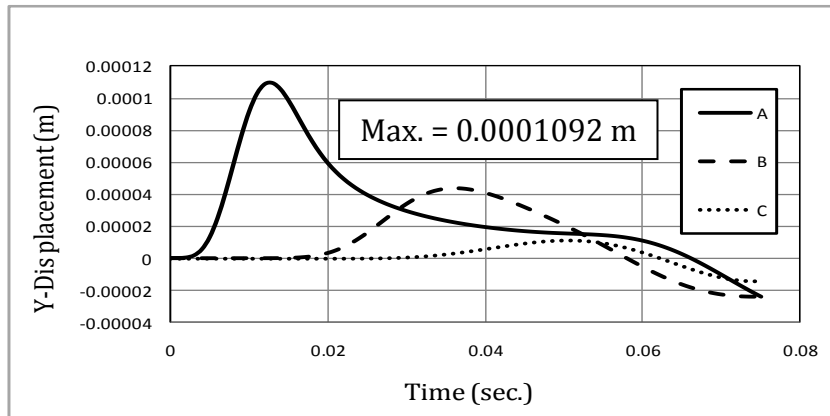
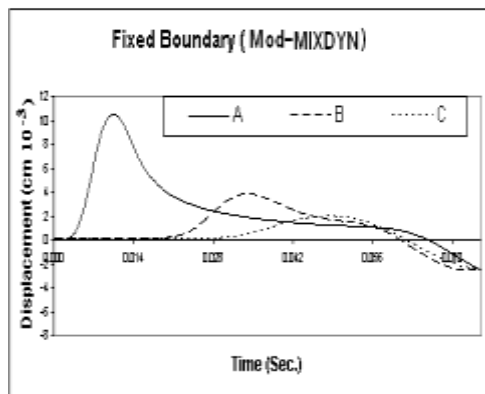


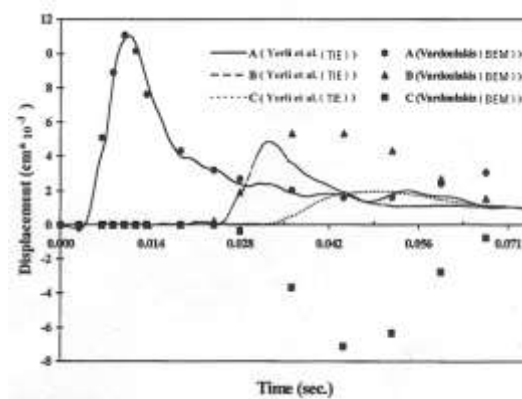
Figure (4) - Cyclic number ratio N/N_L versus pore pressure ratio r_u (after Seed and Booker, 1977).



(a) QUAKE/W program.



(b) Dawood (2006)



(c) Yerli et al., (1998)

Figure (5) - Displacement versus time at points A, B and C.

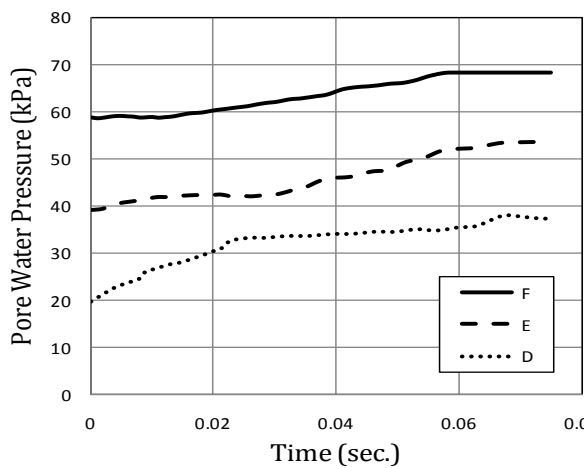


Figure (6) -Pore water pressure time history at points D, E, and F.

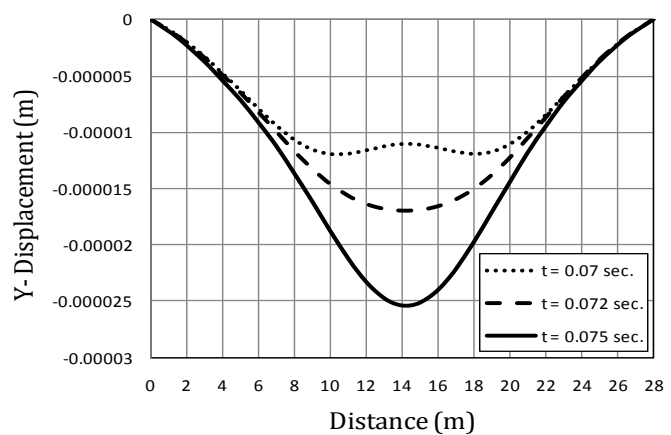


Figure (7) - Surface displacement at different times.

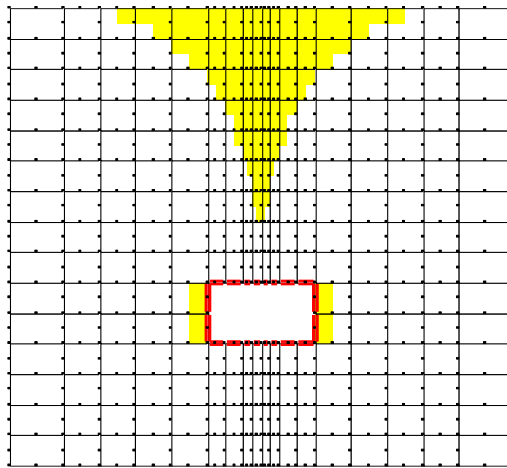


Figure (8) - Liquefaction zones at time (0.075 sec) around underground opening.

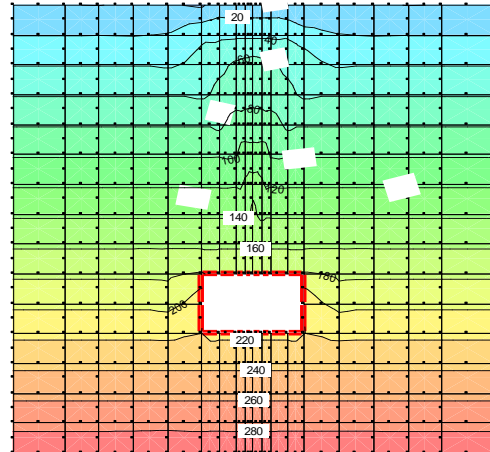


Figure (9) - Contour lines of pore water pressure at time (0.075 sec).

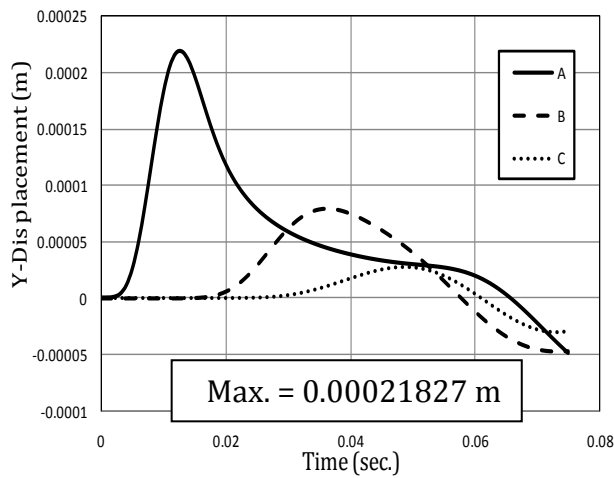


Figure (10) - Displacement time history of points A, B and C under $P_o = 766$ kPa.

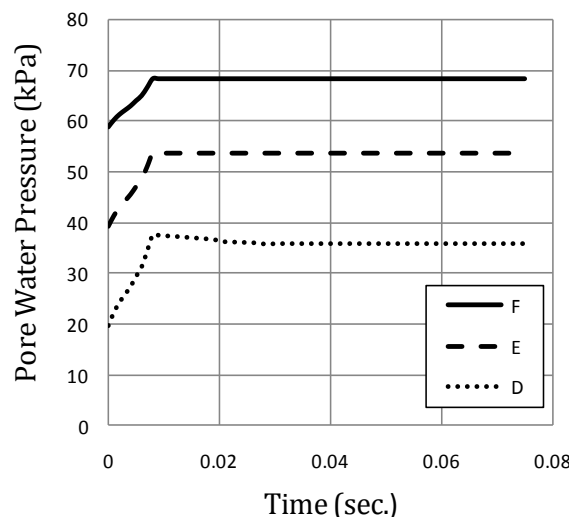


Figure (11) - Pore water pressure time history of points D, E, and F under $P_o = 766$ kPa.

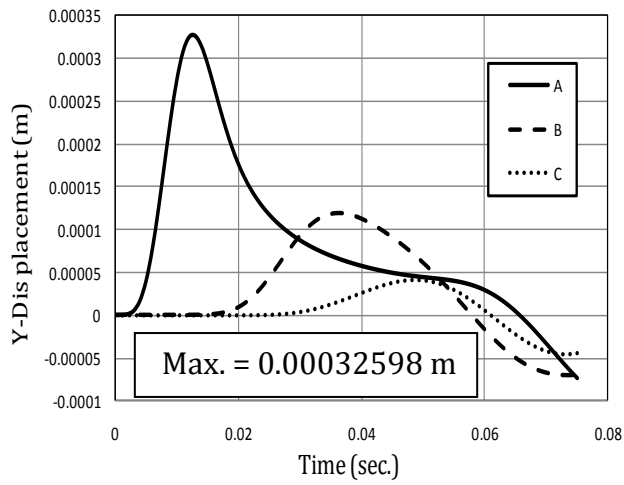


Figure (12) - Displacement time history at points A, B and C under $P_0 = 1150$ kPa .

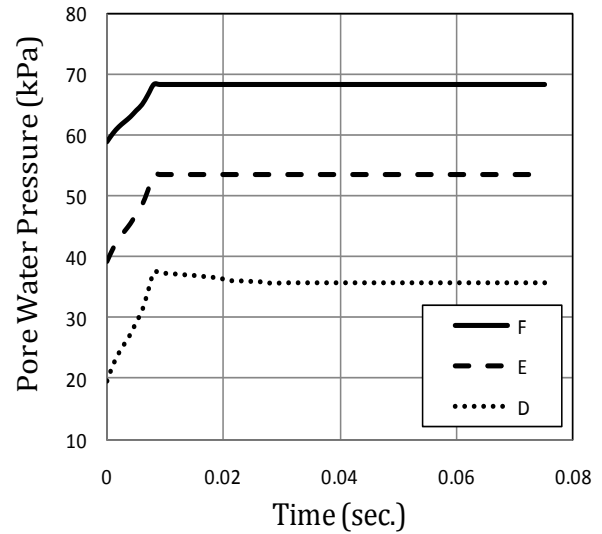


Figure (13) - Pore water pressure time history of points D, E, and F under $P_0 = 1150$ kPa.

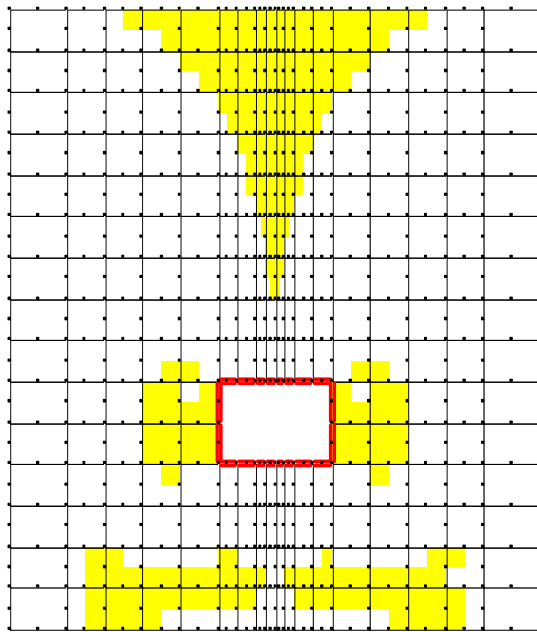


Figure (14) - Liquefaction zones at time (0.075 sec) around underground opening under $P_0 = 766$ kPa.

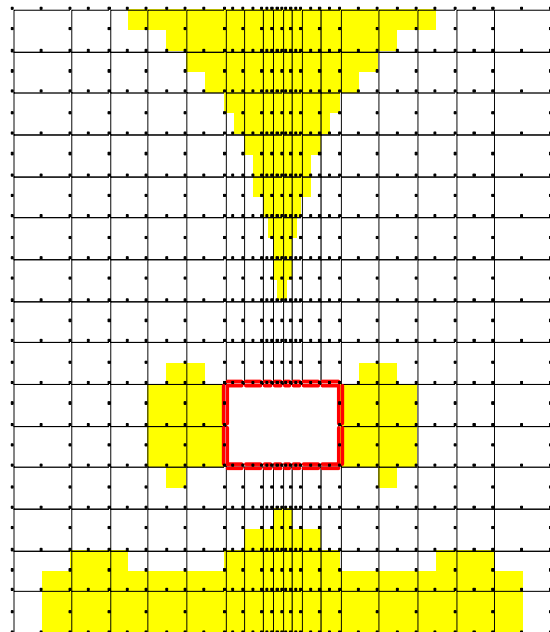


Figure (15) -Liquefaction zones at time (0.075 sec) around underground opening under $P_0 = 1150$ kPa.

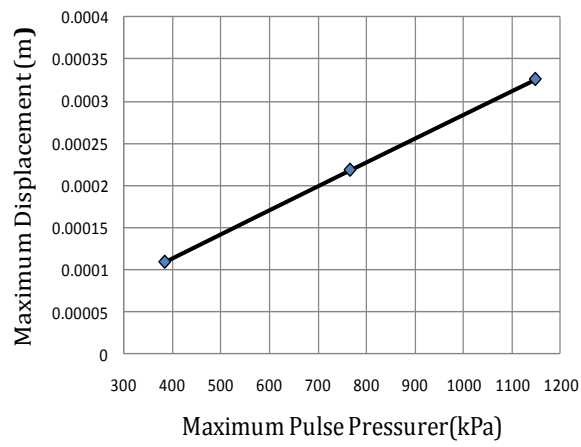


Figure (16) -Maximum surface displacement vs. applied stress at point A.

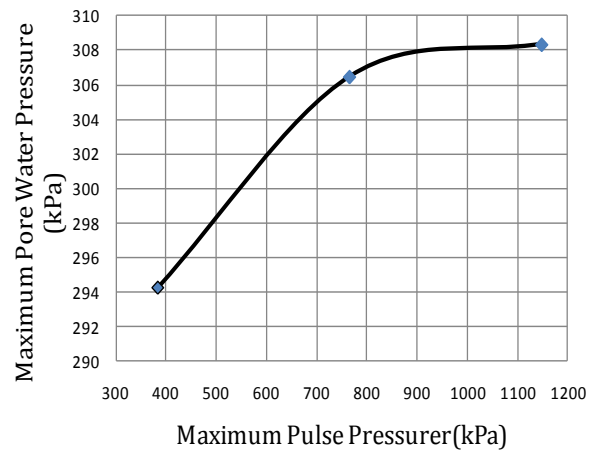


Figure (17) -Maximum pore water pressure vs. applied stress.